

## Kinetics and Mechanism of Complex Formation between $\text{Mg}^{2+}$ and Methylthymol Blue

C. Bremer, H. Ruf, and E. Grell\*

Max-Planck-Institut für Biophysik, Kennedyallee 70, 60596 Frankfurt, Germany

Received: June 25, 1997; In Final Form: October 22, 1997<sup>⊗</sup>

The kinetics of complex formation between Methylthymol Blue (MTB) and  $\text{Mg}^{2+}$  has been investigated between pH 6.15 and 8.0 by laser temperature-jump relaxation spectrometry. In addition to a fast, not time-resolved amplitude change, which is attributed to protolytic reactions, two resolvable relaxation processes have been found in the millisecond time range and are assigned to the binding of  $\text{Mg}^{2+}$  to different protolytic states of MTB. The ratio of the corresponding relaxation times is around 3. From the  $\text{Mg}^{2+}$  concentration and the pH dependence of the slower of the two relaxation times the kinetic parameters related to 1:1 and 1:2 complex formation (MTB: $\text{Mg}^{2+}$ ) have been calculated on the basis of a detailed binding model considering different protolytic states of bound and unbound ligand. The rate constants of complex formation between the ligand's fully deprotonated coordination sites and  $\text{Mg}^{2+}$  are around  $10^7 \text{ M}^{-1} \text{ s}^{-1}$  and are in good agreement with the Eigen–Wilkins mechanism, whereas those between its monoprotonated sites and the cation are of the order of  $5 \times 10^3 \text{ M}^{-1} \text{ s}^{-1}$  and are thus by a factor of about 200 lower than those expected by the Eigen–Wilkins mechanism. This difference is interpreted in molecular terms by assuming that the monoprotonated state of the coordination sites of the ligand is stabilized by intramolecular hydrogen bond formation. Opening of this hydrogen bond is thought to be a rapidly equilibrating step, characterized by an equilibrium constant around 200, preceding the cation coordination. The rate-limiting step of  $\text{Mg}^{2+}$  binding is, in accordance to the Eigen–Wilkins mechanism, still attributed to inner-sphere solvate substitution of the cation.

### Introduction

Kinetic studies in the 1950s about the formation of ligand–metal complexes resulted in the formulation of the so-called Eigen–Wilkins mechanism consisting of three consecutive elementary steps:<sup>1</sup> After a diffusion controlled and thus very fast encounter of the two reactants, the ligand L and the metal M form an outer-sphere complex where at least one solvate molecule within the second coordination sphere of the cation is substituted by the ligand. This step normally proceeds very fast, too. For example, for the binding between electrolytes with bivalent anions and certain cations first-order rate constants of the order of  $10^9 \text{ s}^{-1}$  have been reported.<sup>1</sup> The third reaction step corresponds to the formation of an inner-sphere complex by substituting one or several solvate molecules of the inner coordination sphere of the cation by the coordinating atoms of the ligand. In most of the cases this step is rate limiting. The stronger the solvate binding to the cation, the slower this reaction step. The first-order rate constant  $k_i$  of the formation of the inner-sphere complex is characteristic to the involved cation. For instance,  $k_i$  is about  $1 \times 10^5 \text{ s}^{-1}$  for  $\text{Mg}^{2+}$  but about  $5 \times 10^7 \text{ s}^{-1}$  for the larger  $\text{Ca}^{2+}$  ion.<sup>1</sup> As long as only the inner-sphere substitution of the first solvate molecule is concerned, the rate of this process is not only rate-limiting but also independent of the nature of the ligand.

Because the third step of the Eigen–Wilkins mechanism generally determines the overall rate the two preceding steps can be treated as a single fast preequilibrium<sup>2</sup> characterizing the outer-sphere complex formation. If furthermore the stability of the ligand–cation complex, LM, is sufficiently high, the concentration of the outer-sphere complex can be considered as being in a steady state and thus the complex formation can be described by the simple one-step reaction model.<sup>1</sup> The corre-

sponding rate constants  $k_{\text{on}}$  and  $k_{\text{off}}$  and the macroscopic stability constant of the complex  $K = k_{\text{on}}/k_{\text{off}} = K_o k_i/k_{-i}$  are then related to the first-order rate constants of formation and dissociation of the inner-sphere complex,  $k_i$  and  $k_{-i}$  respectively, and the stability constant of the outer-sphere complex,  $K_o$ , by  $k_{\text{on}} = K_o k_i$  and  $k_{\text{off}} = k_{-i}$ . Assuming spherical molecules and neglecting activity corrections,  $K_o$  can be estimated according to ref 3. It depends, among other parameters, on the charge numbers of the reactants, the mean distance between them in the outer-sphere complex, and the dielectric constant of the solution.

A considerable number of investigations have shown that this mechanism describes in many cases the formation of metal complexes in a consistent manner. On the other hand, there are reactions known that require modifications of this mechanism; some selected ones are discussed by Diebler.<sup>2</sup> Especially the formation of intramolecular hydrogen bonds in chelating ligands can slow the rates of complex formation reactions significantly. As shown by Eigen et al.,<sup>4</sup> intramolecular hydrogen bonds exist even in polar media like water as concluded from the investigation of protolysis of suitable ligands. Additionally, Diebler et al.<sup>5,6</sup> have shown that in the case of the transition metal ions  $\text{Ni}^{2+}$ ,  $\text{Co}^{2+}$ , and  $\text{Zn}^{2+}$  the rate constants of complex formation with substituted salicylic acids are decreased due to intramolecular hydrogen bonding by a factor as high as 4000, compared to what would have to be expected according to the Eigen–Wilkins mechanism.

In the present study, the triphenylmethane dye Methylthymol Blue (MTB; 3,3'-bis[*N,N'*-di(carboxymethyl)aminomethyl]-thymolsulfonphthalein) is chosen as ligand because it acts as a suitable  $\text{Mg}^{2+}$  indicator.<sup>7</sup> The structure of MTB (cf. Figure 1) suggests that MTB exhibits several protolytic equilibria. The fact that there are two almost identical binding sites in MTB for cations, each site consisting of a phenolic oxygen, a tertiary nitrogen, and two carboxylate groups<sup>8</sup> (cf. Figure 1), suggests furthermore that two cations can be bound per molecule of

\* Corresponding author. Tel: (49) 69 6303 290. Fax: (49) 69 6303 346.

<sup>⊗</sup> Abstract published in *Advance ACS Abstracts*, December 1, 1997.

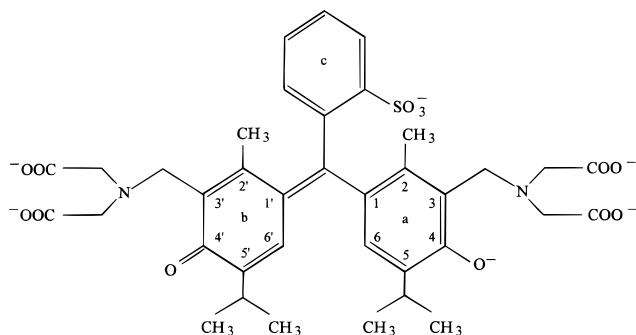


**Figure 1.** Structure of the completely deprotonated state of Methylthymol Blue (MTB; Kekulé notation).

MTB. Potentiometric and spectrophotometric titrations provided experimental evidence for this stoichiometry,<sup>9,10</sup> as well as for the existence of several protolytic states of free MTB and its cation complexes.<sup>9-11</sup>

The purpose of the present study is to examine the kinetics of  $\text{Mg}^{2+}$  binding by MTB at various pH values using the results of equilibrium studies performed earlier<sup>10</sup> and to elucidate the binding mechanism by considering the different protolytic states of MTB. This information is important for establishing MTB as kinetic  $\text{Mg}^{2+}$  indicator in biochemical studies and for the study of the dynamics of photolytic  $\text{Mg}^{2+}$  release from caged compounds.

## Experimental Section

**Materials.** Tetramethylammonium hydroxide (TMAOH; supplied from Fluka; Neu-Ulm) was recrystallized from 2-propanol/diisopropyl ether and tetramethylammonium chloride (TMACl; supplied from Fluka) from ethanol and dried over  $\text{P}_2\text{O}_5$  at 0.01 Torr for 48 h. Hexafluoroacetone trihydrate (HFA; supplied from Fluka) was of purum quality. MTB was purchased from Fluka as tetrasodium salt. The selected batch (186422 76) contained less than 1% of impurities.<sup>10</sup> All other chemicals were of analytical grade, purchased from Merck (Darmstadt) or Fluka and were used without further purification.

**Methods.** All kinetic measurements were performed in thermostated quartz cuvettes with inner dimensions of  $10 \times 2 \text{ mm}^2$  cleaned thoroughly by storing in 5% RBS-35 (Roth; Karlsruhe). The pH values of all examined solutions were buffered employing either 25 mM 2-amino-2-(hydroxymethyl)-1,3-propanediol (= Tris)/HCl (above pH 7.3) or 25 mM HFA/TMAOH (below pH 7.5). The ionic strength of the sample solutions was adjusted to  $I = 0.1 \text{ M}$  with TMACl. The pH of the sample solutions was controlled after the experiments by a specially constructed microelectrode (filled with 3 M KCl, Möller; Zürich) and a pH meter (model 691, Metrohm; Herisau) calibrated at pH 7.00 and pH 4.01 or pH 9.18 by employing standard buffer solutions (Radiometer; Copenhagen). The concentrations of MTB and the cation were verified spectrophotometrically (MCS210, Zeiss; Oberkochen) because the absorption spectra depend characteristically on these concentrations.<sup>10</sup> The temperature of the solutions after the temperature jump was  $25.0 \pm 0.2 \text{ }^\circ\text{C}$ . The temperature of the sample solution was measured by means of a PT100 sensor in combination with a digital thermometer (model 2180A, Fluke; Mountlake Terrace).

The kinetic studies were performed using a laser temperature-jump apparatus described earlier.<sup>12</sup> By absorption of infrared radiation emitted by a pulsed iodine laser (modified IL100, Vuman; Manchester), the temperature of the solution was raised by 1–2  $^\circ\text{C}$  in a volume of about 150 mL within 10  $\mu\text{s}$ . The

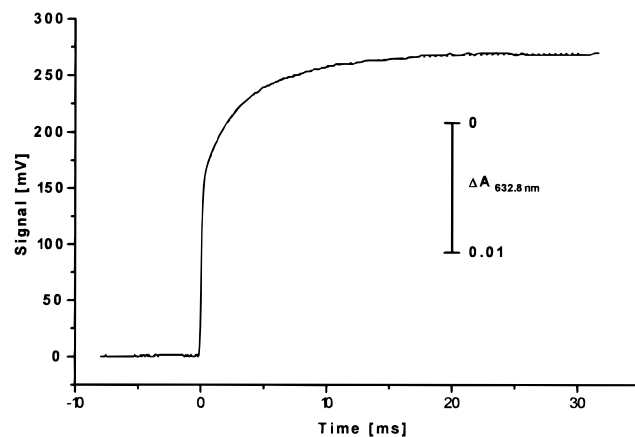


**Figure 2.** Single laser temperature-jump experiment of 0.1 mM MTB and 1 mM  $\text{MgCl}_2$  in 25 mM Tris/HCl, pH 7.3, at 25  $^\circ\text{C}$ , ionic strength 0.1 M (TMACl). The absorption  $A$  at 632.8 nm (rise time filter, 100  $\mu\text{s}$ ; optical path length, 1 cm) is recorded as a function of time. At time  $t = 0$  a heating pulse of 10  $\mu\text{s}$  duration induced a temperature jump of 1.4  $^\circ\text{C}$ . The evaluation provides two resolvable relaxation processes with the relaxation times  $\tau_1 = 1.6 \text{ ms}$  and  $\tau_2 = 5.8 \text{ ms}$ ; the corresponding theoretical curve, drawn as dotted line, is almost indistinguishable from the experimental data. The vertical bar relates the signal to absorbance units.

magnitude of the temperature-jump of each individual experiment was calculated as described elsewhere.<sup>12</sup> The chemical relaxation process induced by the temperature jump was monitored in absorption (optical path length: 1 cm) using a HeNe laser with a specially stabilized power supply (GLG5741, NEC; Tokyo) and a detector based on a silicon photodiode (S1722-02; Hamamatsu, Hamamatsu City).<sup>13</sup> Its signal and that of a reference detector, based on a photomultiplier (1p28; RCA, Lancaster),<sup>14</sup> were amplified to 5.00 V by means of a control desk (DIA-RQC, Dialog; Düsseldorf). The difference of these signals was formed and high-frequency noise removed by a low-pass filter with a suitable rise time being at least a factor of 10 below the relaxation time of the observed process. The resulting data were stored on a transient recorder (Model 4500, Gould; Santa Clara) and evaluated in terms of a sum of decaying exponentials with individual amplitudes by the program DISCRETE 1B.<sup>15</sup> The resulting, averaged relaxation times are obtained from at least four individual experiments with each solution. The evaluation of the dependence of the mean reciprocal relaxation times on concentrations as well as that of the dependence of the apparent rate constants on pH was performed by a special fit program. This program is based on a Gaussian nonlinear least-squares algorithm employing for a given number of trials a random variation of the starting values of the parameters to be determined from those which were entered initially by the user. The parameters resulting during these trials from that evaluation, which yielded the least  $\chi^2$  value of the fit, were taken as estimations of the corresponding true values.

## Results

As a typical example of the time-dependent absorption signals obtained in a single temperature-jump experiment Figure 2 shows the relaxation of the chemical system consisting of 0.1 mM MTB, 1 mM  $\text{MgCl}_2$  and 25 mM Tris/HCl pH 7.3 at 25  $^\circ\text{C}$  (ionic strength 0.1 M adjusted by TMACl) after a temperature jump of 1.4  $^\circ\text{C}$ . The induced shift of the chemical equilibrium could be followed at 632.8 nm in absorption with a root-mean-square noise of about  $2 \times 10^{-4}$  of the total detector signal. The recorded relaxation curve consists of a time-resolvable contribution and of an amplitude change occurring already within the

**TABLE 1: Reciprocal Relaxation Times  $1/\tau_1$  and  $1/\tau_2$  Obtained from Data of Temperature-Jump Experiments of 0.1 mM MTB, Different Concentrations of  $\text{MgCl}_2$  ( $c_{\text{M0}}$ ), 25 mM Buffer (1, HFA/TMAOH; 2, Tris/HCl) at Various pH Values ( $\pm 0.05$ ) at an Ionic Strength of 0.1 M (TMACl), 25 °C<sup>a</sup>**

| $c_{\text{M0}}$ (M) | $1/\tau_1$ and $1/\tau_2$ (s <sup>-1</sup> ) | pH, buffer |            |            |           |          |         |          |
|---------------------|--|------------|------------|------------|-----------|----------|---------|----------|
|                     |  | 6.15, 1    | 6.50, 1    | 6.90, 1    | 7.30, 1   | 7.30, 2  | 7.65, 2 | 8.00, 2  |
| 0.0003              | $1/\tau_1$                                   |            |            | 850 ± 140  |           |          |         |          |
|                     | $1/\tau_2$                                   |            |            | 260 ± 60   |           |          |         |          |
| 0.001               | $1/\tau_1$                                   |            |            | 1000 ± 70  | 680 ± 7   | 130 ± 1  | 120 ± 1 | 50 ± 1   |
|                     | $1/\tau_2$                                   |            |            | 280 ± 7    | 180 ± 5   | 150 ± 1  | 130 ± 1 | 70 ± 1   |
| 0.003               | $1/\tau_1$                                   | 2400 ± 400 | 2100 ± 140 | 1200 ± 70  |           |          |         |          |
|                     | $1/\tau_2$                                   | 400 ± 110  | 510 ± 30   | 320 ± 5    |           | 220 ± 1  | 200 ± 1 | 130 ± 1  |
| 0.004               | $1/\tau_1$                                   |            |            |            | 800 ± 6   |          |         |          |
|                     | $1/\tau_2$                                   |            |            |            | 250 ± 7   |          |         |          |
| 0.006               | $1/\tau_1$                                   | 2700 ± 400 | 1900 ± 80  | 1500 ± 90  |           |          |         |          |
|                     | $1/\tau_2$                                   | 610 ± 40   | 550 ± 10   | 400 ± 5    |           | 290 ± 1  | 280 ± 1 | 240 ± 2  |
| 0.007               | $1/\tau_1$                                   |            |            |            | 910 ± 8   |          |         |          |
|                     | $1/\tau_2$                                   |            |            |            | 310 ± 15  |          |         |          |
| 0.009               | $1/\tau_1$                                   | 2750 ± 150 | 1900 ± 70  | 1300 ± 70  |           |          |         |          |
|                     | $1/\tau_2$                                   | 680 ± 50   | 590 ± 10   | 440 ± 8    |           | 350 ± 1  | 370 ± 1 | 320 ± 4  |
| 0.010               | $1/\tau_1$                                   |            |            |            | 1420 ± 15 |          |         |          |
|                     | $1/\tau_2$                                   |            |            |            | 410 ± 35  |          |         |          |
| 0.012               | $1/\tau_1$                                   | 2900 ± 300 | 2700 ± 130 | 1500 ± 70  |           |          |         |          |
|                     | $1/\tau_2$                                   | 700 ± 50   | 660 ± 10   | 490 ± 7    |           | 430 ± 2  | 450 ± 3 | 430 ± 7  |
| 0.013               | $1/\tau_1$                                   |            |            |            | 1620 ± 30 |          |         |          |
|                     | $1/\tau_2$                                   |            |            |            | 490 ± 60  |          |         |          |
| 0.015               | $1/\tau_1$                                   | 2840 ± 140 | 2600 ± 150 | 2600 ± 200 |           |          |         |          |
|                     | $1/\tau_2$                                   | 750 ± 20   | 690 ± 10   | 610 ± 5    |           | 540 ± 4  | 490 ± 3 | 540 ± 10 |
| 0.016               | $1/\tau_1$                                   |            |            |            | 2420 ± 15 |          |         |          |
|                     | $1/\tau_2$                                   |            |            |            | 580 ± 40  |          |         |          |
| 0.018               | $1/\tau_1$                                   | 2950 ± 130 | 2500 ± 130 | 2700 ± 190 |           |          |         |          |
|                     | $1/\tau_2$                                   | 770 ± 20   | 730 ± 10   | 660 ± 6    |           | 600 ± 4  | 550 ± 5 | 600 ± 10 |
| 0.019               | $1/\tau_1$                                   |            |            |            | 2290 ± 15 |          |         |          |
|                     | $1/\tau_2$                                   |            |            |            | 620 ± 30  |          |         |          |
| 0.021               | $1/\tau_1$                                   | 3160 ± 180 | 2700 ± 160 | 2000 ± 150 |           |          |         |          |
|                     | $1/\tau_2$                                   | 810 ± 20   | 780 ± 10   | 670 ± 9    |           | 690 ± 3  | 700 ± 8 | 700 ± 20 |
| 0.022               | $1/\tau_1$                                   |            |            |            | 2150 ± 20 |          |         |          |
|                     | $1/\tau_2$                                   |            |            |            | 690 ± 60  |          |         |          |
| 0.024               | $1/\tau_1$                                   | 3240 ± 150 |            | 2800 ± 240 |           |          |         |          |
|                     | $1/\tau_2$                                   | 810 ± 30   |            | 760 ± 8    |           |          | 630 ± 5 |          |
| 0.025               | $1/\tau_1$                                   |            | 2900 ± 160 |            | 2710 ± 25 |          |         |          |
|                     | $1/\tau_2$                                   |            | 820 ± 10   |            | 720 ± 70  | 850 ± 14 |         | 730 ± 20 |
| 0.027               | $1/\tau_1$                                   | 3400 ± 160 |            | 2600 ± 220 | 2310 ± 40 |          |         |          |
|                     | $1/\tau_2$                                   | 840 ± 30   |            | 780 ± 9    | 720 ± 70  |          | 670 ± 8 |          |
| 0.030               | $1/\tau_1$                                   | 3800 ± 300 | 2200 ± 110 |            |           |          |         |          |
|                     | $1/\tau_2$                                   | 820 ± 30   | 830 ± 20   |            |           | 880 ± 12 |         | 670 ± 15 |

<sup>a</sup> Averaged values resulting from at least four single temperature-jump experiments are given.

short heating period. The fast amplitude change is observed also in the absence of  $\text{MgCl}_2$  and is due to the rapidly equilibrating protolytic reactions of the chemical system in buffered solution. It is mainly caused by the marked temperature dependence of the protolytic equilibrium of the Tris/HCl buffer,<sup>16</sup> which equilibrates under the chosen experimental conditions within very short times well below the millisecond time range<sup>1</sup> and is monitored by means of the pH dependence of the absorption spectrum of MTB and its  $\text{Mg}^{2+}$  complexes.<sup>10</sup> The time-resolvable part of the relaxation is well described by two decaying exponentials and thus by two relaxation processes with relaxation times  $\tau_1 = 1.6$  ms and  $\tau_2 = 5.8$  ms, but not by a single decaying exponential.

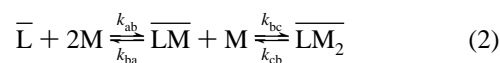
Similar temperature-jump experiments were performed at different total  $\text{Mg}^{2+}$  concentrations ranging from 0.3 to 30 mM and at different pH values between 6.15 and 8.0. The averaged reciprocal relaxation times found in these temperature-jump experiments are summarized in Table 1. Below pH 7.5 the relaxation signals had to be analyzed by two resolvable processes with relaxation times ranging between 0.25 and 5.6 ms. Under all experimental conditions the longer time ( $\tau_2$ ) was only about 3 times larger than the shorter one ( $\tau_1$ ). Both relaxation times decreased with increasing  $\text{Mg}^{2+}$  concentration at constant pH and increased with increasing pH at constant  $\text{Mg}^{2+}$  concentra-

tion. The ratio of the amplitude of the faster over that of the slower resolved relaxation process decreased with increasing pH at a given  $\text{Mg}^{2+}$  concentration. Thus, above pH 7.5 generally only the slower relaxation process with relaxation times between 1 and 20 ms could be detected directly. As an example of the dependence of the reciprocal relaxation time  $1/\tau_2$  on the  $\text{Mg}^{2+}$  concentration the data obtained at pH 7.65 are shown graphically in Figure 3.

Because two time-resolvable relaxation processes with characteristic  $\text{Mg}^{2+}$  concentration dependencies of the corresponding reciprocal relaxation times are observed, the simple one-step reaction scheme



is not sufficient to describe binding of  $\text{Mg}^{2+}$  to MTB even at constant pH. Spectrophotometric  $\text{Mg}^{2+}$  titrations have indicated<sup>9,10</sup> that also formation of complexes with 1:2 stoichiometry (ligand:cation) must be considered:



The upper bar denotes the sum of all protolytic states of the

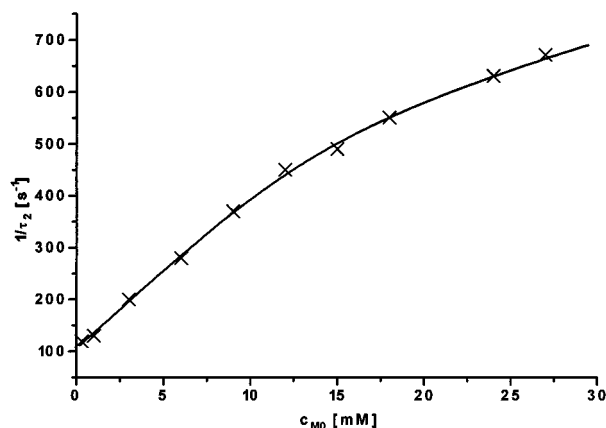


**Figure 3.** Temperature-jump experiments with 0.1 mM MTB at different concentrations of MgCl<sub>2</sub> ( $c_{M0}$ ) in 25 mM Tris/HCl pH 7.65, at 25 °C, adjusted to an ionic strength of 0.1 M (TMACl): Plot of the reciprocal slower relaxation time ( $1/\tau_2$ ) versus  $c_{M0}$ . The solid line represents the theoretical dependence according to model 2 with apparent rate constants  $k_{ab} = (3.3 \pm 0.1) \times 10^4 \text{ M}^{-1} \text{ s}^{-1}$ ,  $k_{ba} = (4.0 \pm 0.2) \times 10^4 \text{ s}^{-1}$ ,  $k_{bc} = (2.5 \pm 0.2) \times 10^4 \text{ M}^{-1} \text{ s}^{-1}$ , and  $k_{cb} = (3.7 \pm 0.3) \times 10^2 \text{ s}^{-1}$ , as calculated by the fitting procedure described in the text.

ligand L and its cation complexes LM and LM<sub>2</sub>, respectively. Hence, the apparent rate constants  $k_{ab}$ ,  $k_{ba}$ ,  $k_{bc}$ , and  $k_{cb}$  depend in general on pH. These rate constants define overall stability constants,  $\overline{K}_1$  and  $\overline{K}_2$ , corresponding to the sums of protolytic states:

$$\overline{K}_1 = \frac{k_{ab}}{k_{ba}} = \frac{c_{\overline{LM}}}{c_{\overline{L}} c_M} \quad (3a)$$

$$\overline{K}_2 = \frac{k_{bc}}{k_{cb}} = \frac{c_{\overline{LM}_2}}{c_{\overline{LM}} c_M} \quad (3b)$$

Protolytic equilibria involved in the chemical system described by eq 2 will not lead to a resolvable relaxation process because the expected relaxation times will be considerably faster than in the millisecond time range<sup>1</sup> under the chosen experimental conditions. Therefore, such equilibria do not have to be considered explicitly in scheme 2.

According to eq 2 two relaxation processes are predicted. Because the experimentally observed, time-resolvable relaxation times differ only by a factor of 3, the reciprocal relaxation times under the condition of strong coupling between the two equilibrium processes are described by the general expression<sup>17</sup>

$$\frac{1}{\tau_{1,2}} = \frac{1}{2} \left[ -(a_{11} + a_{22}) \pm \sqrt{(a_{11} + a_{22})^2 - 4(a_{11}a_{22} - a_{12}a_{21})} \right] \quad (4)$$

with the positive sign of the square root term corresponding to the reciprocal of the faster relaxation time  $\tau_1$ , its negative sign to  $\tau_2$ , and the coefficients  $a_{ij}$  ( $i, j = 1, 2$ ) being defined by

$$a_{11} = -k_{ba} - k_{ab}(c_{\overline{L}} + c_M) \quad (5a)$$

$$a_{12} = -k_{ba} + k_{ab}c_{\overline{L}} \quad (5b)$$

$$a_{21} = k_{bc}(c_{\overline{LM}} - c_M) \quad (5c)$$

$$a_{22} = -k_{cb} - k_{bc}(c_{\overline{LM}} + c_M) \quad (5d)$$

Since the expressions given in eq 4 depend both for  $1/\tau_1$  as well as for  $1/\tau_2$  on all four individual rate constants via the coefficients  $a_{ij}$ , the complete set of rate constants involved in the reaction model specified in eq 2 can be determined under certain conditions<sup>17</sup> from the concentration dependence of either reciprocal relaxation time. The equilibrium concentrations of the free ligand, of the 1:1 complex, and of the 1:2 complex, each being the sum of a number of different protolytic states, are given by the total concentrations of MTB ( $c_{L0} = 0.1 \text{ mM}$ ) and Mg<sup>2+</sup> ( $c_{M0}$ ; varying between 0.3 and 30 mM in this study) according to<sup>10</sup>

$$c_{\overline{L}} = \frac{c_{L0}}{1 + c_M \overline{K}_1 (1 + c_M \overline{K}_2)} \quad (6a)$$

$$c_{\overline{LM}} = c_{\overline{L}} c_M \overline{K}_1 \quad (6b)$$

$$c_{\overline{LM}_2} = c_{\overline{LM}} c_M \overline{K}_2 \quad (6c)$$

using the equilibrium concentration of the unbound cation  $c_M$ . This concentration is the solution of the equation<sup>10</sup>

$$0 = c_M^3 + c_M^2 \left( 2c_{L0} - c_{M0} + \frac{1}{\overline{K}_2} \right) + c_M \left( c_{L0} - c_{M0} + \frac{1}{\overline{K}_1} \right) \frac{1}{\overline{K}_2} - \frac{c_{M0}}{\overline{K}_1 \overline{K}_2} \quad (7)$$

The data of the reciprocal slower relaxation times,  $1/\tau_2$ , obtained at constant pH value but different total Mg<sup>2+</sup> concentrations (see Table 1) were evaluated on the basis of eqs 4–7. The apparent rate constants defined by the scheme in eq 2, which resulted from this evaluation, are compiled in Table 2. In addition, for pH values below 7.5 the reciprocal relaxation times of the faster process were evaluated for control purposes employing expression 4 for  $1/\tau_1$  (results not shown). Although in these latter evaluations the apparent rate constants could be determined with much less accuracy due to small amplitudes of this relaxation process, the resulting apparent rate constants are within experimental errors equal to those calculated from the slowest relaxation times.

As expected already from the spectrophotometric Mg<sup>2+</sup> titrations,<sup>10</sup> all apparent rate constants given in Table 2 depend on pH. This indicates that all states of the ligand in the scheme expressed in eq 2 consist indeed of more than one protolytic

**TABLE 2: Apparent Formation and Dissociation Rate Constants Obtained According to the Model Given in Eq 2 from the Dependence of  $1/\tau_2$  on the Total MgCl<sub>2</sub> Concentration Investigated at Different pH Values, as Given in Table 1 (Ionic Strength, 0.1 M; 25 °C; Buffer 1, 25 mM HFA/TMAOH; Buffer 2, 25 mM Tris/HCl)**

| pH          | buffer | $k_{ab}$ (M <sup>-1</sup> s <sup>-1</sup> ) | $k_{ba}$ (s <sup>-1</sup> )    | $k_{bc}$ (M <sup>-1</sup> s <sup>-1</sup> ) | $k_{cb}$ (s <sup>-1</sup> )   |
|-------------|--------|---|--------------------------------|---|-------------------------------|
| 6.15 ± 0.05 | 1      | (1.3 ± 0.2) × 10 <sup>4</sup>               | (5.5 ± 0.3) × 10 <sup>2</sup>  | (2 ± 57) × 10 <sup>2</sup>                  | (8.3 ± 0.2) × 10 <sup>2</sup> |
| 6.50 ± 0.05 | 1      | (1.6 ± 0.1) × 10 <sup>4</sup>               | (4.5 ± 0.1) × 10 <sup>2</sup>  | (0.6 ± 0.8) × 10 <sup>2</sup>               | (8.4 ± 0.2) × 10 <sup>2</sup> |
| 6.90 ± 0.05 | 1      | (2.4 ± 0.2) × 10 <sup>4</sup>               | (2.5 ± 0.1) × 10 <sup>2</sup>  | (2 ± 15) × 10 <sup>3</sup>                  | (8.5 ± 2.8) × 10 <sup>2</sup> |
| 7.30 ± 0.05 | 1      | (3.0 ± 0.3) × 10 <sup>4</sup>               | (1.5 ± 0.05) × 10 <sup>2</sup> | (6.8 ± 1.6) × 10 <sup>3</sup>               | (6.6 ± 0.2) × 10 <sup>2</sup> |
| 7.30 ± 0.05 | 2      | (2.7 ± 0.3) × 10 <sup>4</sup>               | (1.3 ± 0.03) × 10 <sup>2</sup> | (7 ± 14) × 10 <sup>3</sup>                  | (11 ± 2) × 10 <sup>2</sup>    |
| 7.65 ± 0.05 | 2      | (3.3 ± 0.1) × 10 <sup>4</sup>               | (1.0 ± 0.02) × 10 <sup>2</sup> | (8.4 ± 2.3) × 10 <sup>3</sup>               | (5.1 ± 0.4) × 10 <sup>2</sup> |
| 8.00 ± 0.05 | 2      | (3.7 ± 0.7) × 10 <sup>4</sup>               | (4.2 ± 0.2) × 10 <sup>1</sup>  | (2.5 ± 0.2) × 10 <sup>4</sup>               | (3.7 ± 0.3) × 10 <sup>2</sup> |

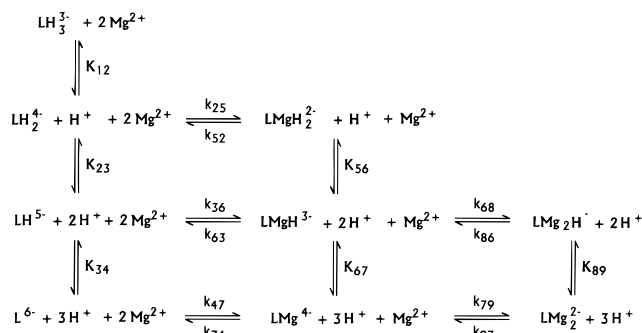


**Figure 4.** Kinetic reaction model of protolysis (columns) and complex formations (rows) between  $\text{Mg}^{2+}$  and MTB existing in different protolytic states. The completely deprotonated state  $\text{L}^{6-}$  of free MTB does not exist to an appreciable amount in the pH range between 6.0 and 8.5. In this pH range the states  $\text{LH}_3^{3-}$ ,  $\text{LH}_2^{4-}$ ,  $\text{LMgH}_2^{2-}$ ,  $\text{LMgH}^{3-}$ , and  $\text{LMg}_2^{2-}$  are the most populated ones.

state. On the basis of the reaction scheme of  $\text{Mg}^{2+}$  binding to MTB proposed earlier<sup>10</sup> (cf. Figure 4), the observed variation of the apparent rate constants with pH can be explained. The concentration of  $\text{L}^{6-}$  (Figure 4) is neglectable as a result of an estimation relating the magnitude of the equilibrium constants  $K_{34}$  and  $K_{67}$ <sup>10</sup> and the investigated pH range. Additionally, one can assume according to ref 3 that  $k_{47}$  is only about 10 times larger than  $k_{36}$  due to the different charges of the corresponding ligand states. Therefore, the reaction path via  $\text{L}^{6-}$  is disregarded. Assuming that equilibration of all protolytic reactions proceeds very rapidly compared to the binding reactions, the apparent rate constants specified in the model given in eq 2 are expressed in terms of the proton concentration,  $c_{\text{H}}$ , of the protolytic equilibrium constants and of the rate constants of the individual binding reactions shown in Figure 4 according to

$$k_{\text{ab}} = \frac{k_{25} + k_{36}/(c_{\text{H}}K_{23})}{1 + c_{\text{H}}K_{12} + 1/(c_{\text{H}}K_{23})} \quad (8a)$$

$$k_{\text{ba}} = \frac{k_{52}c_{\text{H}}K_{56} + k_{63}}{1 + c_{\text{H}}K_{56} + 1/(c_{\text{H}}K_{67})} \quad (8b)$$

$$k_{\text{bc}} = \frac{k_{68} + k_{79}/(c_{\text{H}}K_{67})}{1 + c_{\text{H}}K_{56} + 1/(c_{\text{H}}K_{67})} \quad (8c)$$

$$k_{\text{cb}} = \frac{k_{86}c_{\text{H}}K_{89} + k_{97}}{1 + c_{\text{H}}K_{89}} \quad (8d)$$

where  $c_{\text{H}}$  is determined by the pH according to  $c_{\text{H}} = 10^{-\text{pH}}$  [M].

The evaluation of the data compiled in Table 2 according to eqs 8 reveals estimates of the rate constants of the individual binding reactions (cf. Table 3) as well as of the corresponding protolytic stability constants  $K_{12} = (2.0 \pm 0.1) \times 10^6 \text{ M}^{-1}$ ,  $K_{56} = (5.1 \pm 1.4) \times 10^6 \text{ M}^{-1}$  (mean value obtained from the

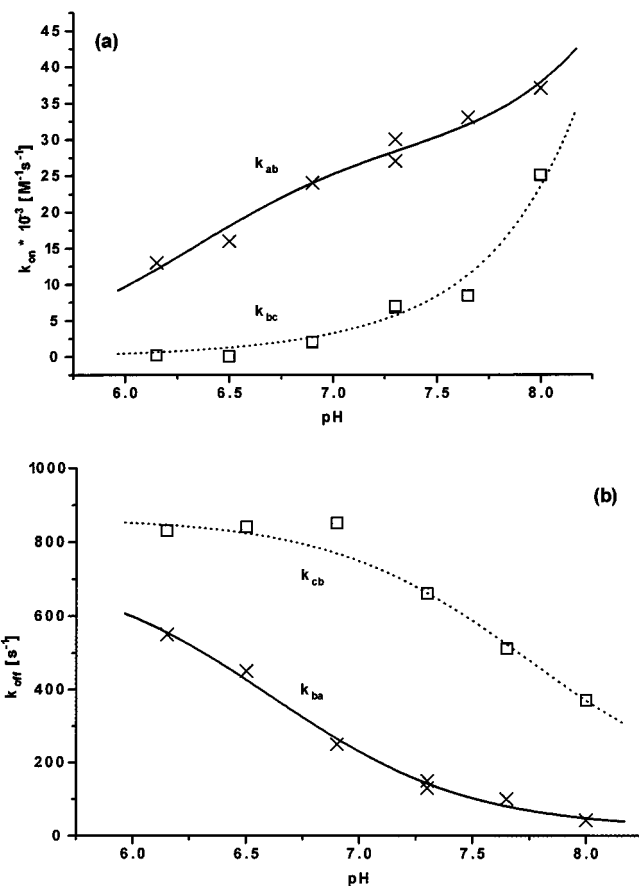


**Figure 5.** Plot of the apparent rate constants (cf. Table 2) of formation ( $k_{\text{on}}$ ; part a) and dissociation ( $k_{\text{off}}$ ; part b) versus pH and of the corresponding theoretical dependencies according to the proposed reaction model (Figure 4) obtained by the fitting procedure described in the text employing eqs 8: (a) crosses and continuous line,  $k_{\text{ab}}$ ; squares and dotted line,  $k_{\text{bc}}$ ; (b) crosses and continuous line,  $k_{\text{ba}}$ ; squares and dotted line,  $k_{\text{cb}}$ . The pH independent rate constants and the protolytic stability constants required for the calculations are given in Table 3 and the text, respectively.

evaluations of  $k_{\text{ba}}$  and  $k_{\text{bc}}$ ), and  $K_{89} = (5.5 \pm 1.3) \times 10^7 \text{ M}^{-1}$ . For this evaluation the protolytic equilibrium constants  $K_{23}$  and  $K_{67}$  were treated as fixed parameters with values of  $1 \times 10^{11} \text{ M}^{-1}$  and  $2.5 \times 10^{10} \text{ M}^{-1}$ , respectively, which have been determined earlier from spectrophotometric titrations.<sup>10</sup> The results of these evaluations are shown graphically in Figure 5. The values of the protolytic stability constants presented here are comparable to those reported earlier.<sup>10</sup> The estimated values of the stability constants of the  $\text{Mg}^{2+}$  complexes with MTB,  $K_{25} = 4 \times 10^1 \text{ M}^{-1}$ ,  $K_{36} = 5 \times 10^5 \text{ M}^{-1}$ ,  $K_{68} = 4 \text{ M}^{-1}$ , and  $K_{79} = 6 \times 10^4 \text{ M}^{-1}$ , which have been calculated from the kinetic parameters determined in this study as the ratio of the rate constant of formation over the corresponding one for dissociation, are up to 1 decade lower than those resulting from equilibrium experiments.<sup>10</sup> The values of stability constants

**TABLE 3: Rate Constants of Complex Formation and Dissociation between  $\text{Mg}^{2+}$  and Different Protolytic States of MTB and Its 1:1 Complexes at 25 °C<sup>a</sup>**

| step | reaction  | complex formation  | complex dissociation                                |
|------|---|--|---|
| 2↔5  | $\text{LH}_2^{4-} + \text{Mg}^{2+} \rightleftharpoons \text{LMgH}_2^{2-}$     | $k_{25} = (2.9 \pm 0.2) \times 10^4 \text{ M}^{-1} \text{ s}^{-1}$ | $k_{52} = (7.4 \pm 0.8) \times 10^2 \text{ s}^{-1}$ |
| 3↔6  | $\text{LH}^{5-} + \text{Mg}^{2+} \rightleftharpoons \text{LMgH}^{3-}$         | $k_{36} = (9.3 \pm 4.4) \times 10^6 \text{ M}^{-1} \text{ s}^{-1}$ | $k_{63} = (1.9 \pm 0.7) \times 10^1 \text{ s}^{-1}$ |
| 6↔8  | $\text{LMgH}^{3-} + \text{Mg}^{2+} \rightleftharpoons \text{LMg}_2\text{H}^-$ | $k_{68} = (3.1 \pm 1.4) \times 10^3 \text{ M}^{-1} \text{ s}^{-1}$ | $k_{86} = (8.6 \pm 0.1) \times 10^2 \text{ s}^{-1}$ |
| 7↔9  | $\text{LMg}^{4-} + \text{Mg}^{2+} \rightleftharpoons \text{LMg}_2^{2-}$       | $k_{79} = (5.5 \pm 0.5) \times 10^6 \text{ M}^{-1} \text{ s}^{-1}$ | $k_{97} = (9.5 \pm 7.9) \times 10^1 \text{ s}^{-1}$ |

<sup>a</sup> The data are determined by a fitting procedure according to eqs 8 on the basis of the values of the apparent rate constants (Table 2) and the proposed reaction model (Figure 4). Details of the evaluation and the corresponding protolytic stability constants are given in the text. The errors reflect the internal consistency of the data.

derived from rate constants are usually much less accurate than the corresponding values determined from equilibrium titrations, in particular when the reaction system is of high complexity as the one suggested here (Figure 4). Nevertheless this scheme, which has been derived on the basis of our kinetic studies, is therefore considered to be compatible with the experimental data of the spectrophotometric equilibrium titrations.<sup>10</sup> This deviation might be only an apparent one due to the fairly large errors of the rate constants, which are a consequence of the large number of parameters pertaining to the minimum reaction scheme shown in Figure 4. Additionally, it is not unusual that values of stability constants calculated from rate constants differ from those determined by equilibrium experiments.

For each apparent rate constant simulation's (not presented here) have been performed according to eqs 8. For these simulations, the complex formation rate constants given in Table 3 have been multiplied by 1, 3, or 10 independently from each other while each complex dissociation rate constant has been divided by 1, 3, or 10. These simulations have shown that simple combinations of rate constants for complex formation or complex dissociation, which would lead to equilibrium constants being comparable to the ones reported earlier,<sup>10</sup> cannot describe the kinetic experiments discussed in this study. Therefore, the discussion will be based mainly on the calculated parameter values compiled in Table 3. These parameter values including their uncertainties reflect the internal consistency of the experimental data with the model shown in Figure 4. Hence, this minimum reaction scheme is compatible with the experimental data both of the kinetic experiments reported here as well as the titrations described earlier.<sup>10</sup>

In addition to the temperature-jump experiments described above, a series of experiments has been performed at pH 8.0 in the presence of different total CaCl<sub>2</sub> concentrations instead of MgCl<sub>2</sub>. The resulting signal changes were much faster than in the case of Mg<sup>2+</sup>. The evaluation of these data allowed to resolve only a single relaxation process. The relaxation time obtained in the presence of 1 mM CaCl<sub>2</sub> (40 μs) is about 350 times lower than in the presence of 1 mM MgCl<sub>2</sub> at pH 8.0 (14 ms). The corresponding relaxation amplitude normalized to a temperature jump of 1 °C is about 3 times larger with CaCl<sub>2</sub> than with MgCl<sub>2</sub>. This is consistent with the stability constants of the cation complexes with MTB<sup>10</sup> which are for Ca<sup>2+</sup> about 3 times lower than those with Mg<sup>2+</sup>. At Ca<sup>2+</sup> concentrations larger than 1 mM the time constant of the observed signal change decreased further approaching the heating time of the apparatus of 10 μs.<sup>12</sup> Therefore, no evaluations have been performed under these conditions.

## Discussion

To develop an interpretation of the experimentally determined rate constants in molecular terms, it is helpful to estimate the effect of the ligand charge on the value of the complex formation constants. To a good approximation only those charges of the ligand that are in the vicinity of the binding site contribute to the equilibrium constant  $K_o$  of the outer-sphere complex (cf. Introduction). The effect of charge on  $K_o$  can be estimated according to ref 3. For spherical molecules and dilute solutions  $K_o$  is approximated by

$$K_o = \frac{4\pi}{3000} r^3 N_A e^{-\Phi} \quad (9a)$$

$$\Phi = \frac{z_+ z_- e_0^2}{4\pi\epsilon_r\epsilon_0 r k_B T} \quad (9b)$$

**TABLE 4: Calculated Formation Rate Constants ( $k_{on}$ ) According to the Eigen–Wilkins Mechanism Using Eqs 9 and  $k_{on} = K_o k_i$  with  $r = 0.6$  nm, Water at 25 °C, and  $k_i = 10^5$  s<sup>-1</sup> for Assumed Effective Charges of the Local Coordinating Sites ( $z_-$ )<sup>a</sup>**

| $z_-$ | $k_{on}$ (M <sup>-1</sup> s <sup>-1</sup> ) | reaction   | step |
|-------|---|--|------|
| -1    | $6 \times 10^5$                             | LMgH <sup>3-</sup> + Mg <sup>2+</sup> → LMg <sub>2</sub> H <sup>-</sup>            | 6→8  |
| -2    | $6 \times 10^6$                             | LH <sub>2</sub> <sup>4-</sup> + Mg <sup>2+</sup> → LMgH <sub>2</sub> <sup>2-</sup> | 2→5  |
|       |   | LMg <sup>4-</sup> + Mg <sup>2+</sup> → LMg <sub>2</sub> <sup>2-</sup>              | 7→9  |
| -3    | $7 \times 10^7$                             | LH <sup>5-</sup> + Mg <sup>2+</sup> → LMgH <sup>3-</sup>                           | 3→6  |

<sup>a</sup> The  $k_{on}$  are assigned to Mg<sup>2+</sup> complex formation rate constants of specified partial reaction steps, as indicated in the reaction scheme shown in Figure 4.

with  $r$  being the mean distance between the reactants in the outer-sphere complex,  $N_A$  the Avogadro number,  $z_+$  and  $z_-$  the charge numbers of the cation and the ligand, respectively,  $e_0$  the elementary charge,  $\epsilon_r\epsilon_0$  the dielectric constant of the solution,  $k_B$  the Boltzmann constant, and  $T$  the absolute temperature. Concerning the system of this study the mean distance cannot be much smaller than the sum of the ionic radius of Mg<sup>2+</sup> being 0.08 nm<sup>18</sup> and of the diameter of a water molecule of 0.34 nm,<sup>19</sup> as the character of the reaction distance for the outer-sphere complex implies. On the other hand, this mean distance is influenced also by the spatial distribution of the charges of the local coordinating site of MTB. Therefore, if the charged groups within the binding site are markedly separated from each other, as suggested in the case of MTB by its molecular model, the mean distance will be larger than 0.42 nm. Assuming all charges involved in the coordinating sites (cf. Figure 1) as effective charges, water as solvent, the formation rate constant  $k_i$  of the inner-sphere complex being  $1 \times 10^5$  s<sup>-1</sup> according to ref 1, and the mean distance  $r$  being 0.6 nm, corresponding to 1.5 layers of water between the cation and the point-charges of the ligand, the expected rate constants  $k_{on}$  can be calculated according to eq 9 and  $k_{on} = K_o k_i$ . The obtained values are given in Table 4 for different effective charges of the local coordinating sites corresponding to the binding of Mg<sup>2+</sup> to different states of the ligand (cf. Figure 4).

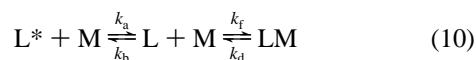
The calculated rate constants  $k_{on}$  (Table 4) can now be compared with the experimentally determined ones (Table 3). As far as the experimentally determined formation rate constants are concerned, it is surprising to note that the values of  $k_{25}$  and  $k_{68}$  are comparable and differ only by about an order of magnitude. However,  $k_{25}$  and  $k_{68}$  are about 2–3 orders of magnitude smaller than  $k_{36}$  and  $k_{79}$  (cf. Table 3), characterizing the binding reactions 3→6 and 7→9, respectively. The values of the latter rate constants (Table 3) agree reasonably well with the expected rate constants (Table 4), which suggests that for these two partial reactions the substitution of the first water molecule of the inner coordination sphere of the cation by the ligand represents the rate-limiting step. The same conclusion applies also in the case of the partial reaction steps 2→5 and 6→8 as indicated by the ratio of the reciprocal relaxation times found at pH 8.0 in the presence of 1 mM CaCl<sub>2</sub> or MgCl<sub>2</sub> (see Results). The value of this ratio is about 350 and is almost equal to that of the ratio of the substitution rate constants  $k_i$  for the Ca<sup>2+</sup> and the Mg<sup>2+</sup> ion<sup>1</sup> ( $5 \times 10^7$  s<sup>-1</sup>/1 × 10<sup>5</sup> s<sup>-1</sup> = 500). On the other hand, the experimentally determined values of  $k_{25}$  and  $k_{68}$  (Table 3) are by a factor of about 200 lower than those estimated according to the values given in Table 4.

These observations can be explained in molecular terms on the basis of a simple model: As already stated by Schwarzenbach and Flaschka,<sup>8</sup> both binding sites of MTB, consisting of the phenolic oxygen, the tertiary nitrogen and the two carboxylate groups, are completely deprotonated (L<sup>6-</sup>; cf. Figure 1)

in the protolytic state exhibiting the strongest interaction with bivalent cations. Depending on pH these coordinating groups can be protonated in the free state as well as, to a certain extent, in the bound state. The dissociation of the phenolic OH group contributes mainly to  $K_{12}$  and that of the protonated amine nitrogen atoms to  $K_{23}$  and  $K_{34}$ , while the carboxylic groups are likely to be deprotonated within the investigated pH range.<sup>10,11</sup> According to this, one of the coordinating atoms in the states  $\text{LMgH}_2^{2-}$  and  $\text{LMg}_2\text{H}^-$  (only one site concerned) is protonated, which is likely to be the amine nitrogen. Thus, the binding reactions 2→5 and 6→8 (cf. Table 3) are essentially identical on the molecular level. The major difference between both partial reactions consists of a charge difference of the sites. The other binding reactions, 3→6 and 7→9, are thus assumed to be characterized by cation coordination to completely deprotonated groups.

The structural considerations on MTB suggest that the protonated nitrogen atom and the phenolic oxygen in its vicinity form an intramolecular hydrogen bond. Additionally, the results and considerations from Diebler et al.<sup>5,6</sup> make this conception plausible. Assuming such an interaction for the states  $\text{LH}_2^{4-}$  and  $\text{LMgH}^{3-}$ , no cation coordination is assumed to take place because two of the four possible binding valences are occupied by the proton. Thus according to this model, the hydrogen bond must open before binding of the cation can occur. The corresponding supposed molecular structures are shown in Figure 6, omitting the groups not involved in the binding reaction.

Thus, we postulate the existence of two microscopic ligand states for  $\text{LH}_2^{4-}$  as well as for  $\text{LMgH}^{3-}$  where only the non hydrogen bonded state **Ib** (cf. Figure 6) is capable to coordinate  $\text{Mg}^{2+}$ . The partial reactions between the cation and  $\text{LH}_2^{4-}$  as well as  $\text{LMgH}_2^{2-}$  and between  $\text{Mg}^{2+}$  and  $\text{LMgH}^{3-}$  as well as  $\text{LMg}_2\text{H}^-$  can then be described by the following general scheme



and the experimentally determined rate constants  $k_{\text{on}}$  and  $k_{\text{off}}$  are given by

$$k_{\text{on}} = \frac{k_f}{1 + K_H} \quad (11a)$$

$$k_{\text{off}} = k_d \quad (11b)$$

$$\text{with } k_f = K_0 k_i \quad (12a)$$

$$\text{and } K_H = k_b/k_a \quad (12b)$$

Here, the rearrangement of the ligand from state  $\text{L}^*$  to state  $\text{L}$  (opening of the hydrogen bond) is assumed to occur fast compared to the binding between the cation  $\text{M}$  and  $\text{L}$ .<sup>20</sup> According to this model the substitution of the first water molecule in the inner coordination sphere of the cation by the ligand represents still the rate-limiting step of the reaction, but the values of the formation rate constants are reduced as the consequence of the existence of an unfavorable preequilibrium due to intramolecular hydrogen bond formation. The equilibrium constant  $K_H$  characterizing the strength of the hydrogen bond is of the order of 200 suggesting that most of the free ligand is present in the state  $\text{L}^*$ , which is unable to coordinate  $\text{Mg}^{2+}$ . This value of  $K_H$  is of the same order as those reported for substituted salicylic acids.<sup>20</sup> However, if we consider the difference between the stability constants of the  $\text{Mg}^{2+}$  complexes

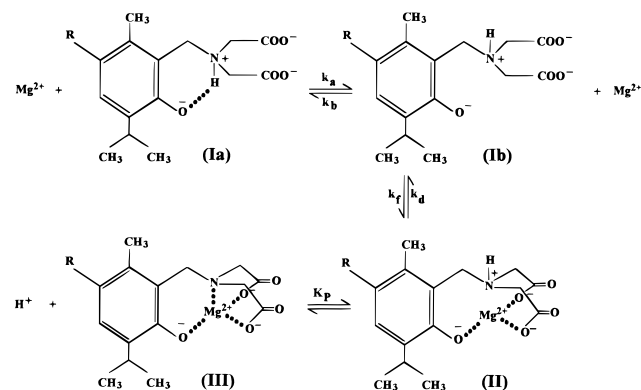


**Figure 6.** Schematic illustration of the proposed partial reaction mechanism for the binding of  $\text{Mg}^{2+}$  to MTB involving an intramolecular hydrogen bond formation as a preequilibrium of cation coordination (one particular resonance structure is shown; the part of the ligand not involved in coordination is summarized by R; hydration is omitted). The structures **Ia** and **Ib** are assigned to the states  $\text{LH}_2^{4-}$  and  $\text{LMgH}^{3-}$  (with and without an intramolecular hydrogen bond formed), structure **II** corresponds to  $\text{LMgH}_2^{2-}$  and  $\text{LMg}_2\text{H}^-$ , and structure **III** corresponds to  $\text{LMgH}^{3-}$  and  $\text{LMg}_2^{2-}$  (cf. Figure 4).  $K_P$  represents  $K_{56}$  or  $K_{89}$ , respectively.

calculated from the rate constants and those reported earlier,<sup>10</sup> the value of  $K_H$  could be up to 10 times smaller.

In summary, the results of the laser pulse induced temperature-jump experiment presented in this study show that between pH 6.15 and 8.0 the kinetics of  $\text{Mg}^{2+}$  binding by MTB can be described by the same model as proposed earlier on the basis of spectrophotometric titrations.<sup>10</sup> In addition, the interpretation of the results of the kinetic experiments provided evidence for the occurrence of an intramolecular hydrogen bond within the coordination site of the protonated states of MTB. The data presented here are then in agreement with the well-established Eigen–Wilkins mechanism. The mechanistic implications resulting from the formation of an intramolecular hydrogen bond may be of importance in biological systems such as enzymatic reactions.

## References and Notes

- (1) Eigen, M. *Z. Elektrochem.* **1960**, *64*, 115.
- (2) Diebler, H. *Habilitation*; University of Göttingen, 1973.
- (3) Fuoss R. M. *J. Am. Chem. Soc.* **1958**, *80*, 5059.
- (4) Eigen, M.; Kruse, W.; Maass, G.; De Maeyer, L. In *Progress in Reaction Kinetics*; Pergamon: Oxford, 1964; Vol. 2, p 287.
- (5) Diebler, H.; Secco, F.; Venturini, M. *J. Phys. Chem.* **1987**, *91*, 5106.
- (6) Diebler, H.; Secco, F.; Venturini, M. *J. Phys. Chem.* **1989**, *93*, 1691.
- (7) Buděšínský, B. In *Chelates in Analytical Chemistry*; Flaschka, H. A., Barnard, A. J., Eds.; Dekker: New York, 1967; Vol. 1, p 15.
- (8) Schwarzenbach, G.; Flaschka, H. *Die komplexometrische Titration*; 5th ed.; Enke: Stuttgart, 1965; p 30.
- (9) Yoshino, T.; Okazaki, H.; Murakami, S.; Kagawa, M. *Talanta* **1974**, *21*, 676.
- (10) Bremer, C.; Grell, E. *Inorg. Chim. Acta* **1996**, *241*, 13.
- (11) Yoshino, T.; Imada, H.; Murakami, S.; Kagawa, M. *Talanta* **1974**, *21*, 211.
- (12) Bremer, C.; Bergbauer, R.; Ruf, H.; Bannister, J. J.; Grell, E. *Meas. Sci. Technol.* **1993**, *4*, 1385.
- (13) Bergbauer, R.; Bremer, C.; Grell, E. *Rev. Sci. Instrum.* **1993**, *64*, 3289.
- (14) Rabl, C. R. Max-Planck-Gesellschaft, Deutsches Bundespatent 23 53 573.
- (15) Provencher, S. W. *J. Chem. Phys.* **1976**, *64*, 580.
- (16) Bates, R. G.; Hetzer, H. B. *J. Phys. Chem.* **1961**, *65*, 667.
- (17) Bremer, C.; Grell, E. *Eur. Biophys. J.* **1994**, *23*, 217.
- (18) Basolo, F.; Pearson, R. G. *Mechanismen in der anorganischen Chemie*; Thieme: Stuttgart, 1973; p 67.
- (19) Freier, R. K. *Aqueous Solutions*; Gruyter: Berlin; 1978; Vol. 2, p 112.
- (20) Diebler, H.; Secco, F.; Venturini, M. *J. Phys. Chem.* **1984**, *88*, 4229.